Appl. Phys. B (2016) 122:62
DOI 10.1007/s00340-016-6332-0

Applied Physics B
Lasers and Optics

Efficient theoretical model and numerical simulation for optimization of gain-switched thulium-doped fiber lasers

Baofu Zhang[1] · Guangyuan He[2] · Zhongxing Jiao[1] · Biao Wang[1]

Received: 7 July 2015 / Accepted: 7 January 2016 / Published online: 12 March 2016

Abstract We demonstrate an effective and simplified theoretical model of the in-band-pumped gain-switched thulium-doped fiber laser in which the effective pump power and effective population density are defined as the approximation of spatial variables. The numerical simulation results based on the model are in good agreement with the experimental data. The parameters of the pump source and the cavity configuration are considered in our numerical model for the optimization of the laser system. The pump condition in which the pulse distortion can be avoided is presented.

1 Introduction

Pulsed 2-μm thulium-doped fiber lasers (TDFLs) are attracting widespread interest in recent years due to their practical applications in medical surgery, environmental detecting and wavelength conversion to mid-infrared through optical parametric oscillations [1–3]. The in-band-pumped gain-switched thulium-doped fiber laser (IGSTDFL) is considered to be an efficient approach to producing 2-μm nanosecond pulses because of its robust all-fiber configuration and flexible performance in nanosecond pulse generation. The all-fiber IGSTDFL systems have been demonstrated by several research groups [4–7].

Gain switching of a laser is typically based on modulating the pump pulse and selecting the first spike of the relaxation oscillation in each lasing period [8, 9]. Therefore, the output pulse characteristics of the gain-switched TDFL are strongly dependent on the pump pulse parameters and cavity geometries. In order to achieve 2-μm short pulses with sufficient pulse energy for meeting the requirements of practical applications, the gain-switched TDFL system should be carefully optimized and its theoretical model is demanded.

Several theoretical models of IGSTDFLs have been reported [10–12]. Zhou et al. [11] obtained the analytical formulations of pump energy threshold, extraction efficiency by solving the rate equations, but there were a few mistakes in their derivation process and few proposals were given for laser system optimization. Moreover, the spatial dependences were not taken into account in their model, which may lead to simulation distortions when the concentration of thulium-doped fiber is high and its length is long. Yang et al. [12] presented their theoretical model in which both temporal and spatial variations were included; they focused on the approach to obtaining laser pulses with Gaussian-like shape and short pulse width. However, the pulse energy, a significant parameter of output laser pulse, was not considered in their model. In addition, their model may be complicated for commercial and engineering applications because a huge number of calculation cycles will be needed to find a relatively steady state of the laser system in their numerical simulation. Compared with the wave traveling model, a modified point model is preferred when applied to practical applications since it can be more efficient.

✉ Zhongxing Jiao
jiaozhx@mail.sysu.edu.cn

✉ Biao Wang
wangbiao@mail.sysu.edu.cn

Baofu Zhang
jkbowry@gmail.com

[1] State Key Laboratory of Optoelectronic Materials and Technologies, School of Physics and Engineering, Sun Yat-sen University, Guangzhou 510275, China

[2] Sino-French Institute of Nuclear Engineering and Technology, Sun Yat-sen University, Guangzhou 510275, China

In this paper, we present an efficient theoretical model of the IGSTDFL in which we define effective pump power and effective population density as the approximation of spatial variables. Results of the numerical simulation based on our model are supported by our previous gain-switched TDFL experiments. The parameters of the pump source and the cavity configuration are considered in our numerical model, for the purpose of achieving stable 2-μm output pulses with short duration and high pulse energy from optimized laser system.

2 Theoretical model

Our theoretical model is based on an in-band-pumped gain-switched thulium-doped silica fiber laser which is a quasi-three-level laser system. This quasi-three-level system can be approximated with a two-level scheme because the transition from the pump band to the upper laser level (both in $^3F_4$ level) is so fast that the population of the pump band is close to zero [8, 9]. Besides, in the TDFL system, the pump power cannot be completely absorbed by the thulium-doped fiber (TDF), and hence, we defined the effective absorbed average pump power in the model by

$$P_{\mathrm{a,\,eff}} = \eta_{\mathrm{a}} P_{\mathrm{a}}, \tag{1}$$

where P_{a} is the launched average pump power produced by the pump source and η_{a} is the absorption efficiency which can be approximated by [8]

$$\eta_{\mathrm{a}} = 1 - \exp[-\alpha(\lambda_{\mathrm{p}}, N_0) l_{\mathrm{f}}], \tag{2}$$

where $\alpha(\lambda_{\mathrm{p}},N_0)$ is the absorption coefficient of the TDF with the Tm^{3+}-ions-doping concentration N_0 (which is also the total population density) at the pump wavelength λ_{p} and l_{f} is the length of the TDF. Moreover, due to the pump absorption effect, the absorbed pump power varies in different segments along the TDF; thus, the spatial variables should be considered in the model. However, according to the rate equation of the three-level solid-state laser system [8, 9], we found that the spatial distributional effect of the absorbed pump power could be approximated by the equivalent reduction in the population which could participate in the lasing process, corresponding to the reduction in the effective population density. Therefore, referring to the effective average pump power, we defined the effective population density in our theoretical model by

$$N_{i,\,\mathrm{eff}} = \eta_{\mathrm{e}} N_i \quad (i = 0, 1, 2), \tag{3}$$

where N_1 and N_2 are the population densities of the lower laser level ($^3H_6$) and the upper laser level ($^3F_4$), respectively. η_{e} is the effective utilization coefficient which can be defined by

$$\eta_{\mathrm{e}} = 1 - \exp\left\{-1/[\alpha(\lambda_{\mathrm{p}}, N_0) l_{\mathrm{f}}]\right\}. \tag{4}$$

Based on the approximations mentioned above and the experimental setup in our previous work [7] (as detailed in Sect. 3), the modified rate equations for our IGSTDFL system can be written as

$$N_{1,\,\mathrm{eff}} + N_{2,\,\mathrm{eff}} = N_{0,\,\mathrm{eff}}, \tag{5}$$

$$\begin{aligned}\frac{\mathrm{d}N_{2,\,\mathrm{eff}}(t)}{dt} = {} & \frac{\Gamma_{\mathrm{p}}\sigma_{\mathrm{a}}P_{\mathrm{a,\,eff}}\varepsilon(t)}{A_{\mathrm{c}}h\nu_{\mathrm{p}}}\left[f_{\mathrm{lp}}N_{1,\,\mathrm{eff}}(t) - f_{\mathrm{up}}N_{2,\,\mathrm{eff}}(t)\right] \\ & - \frac{N_{2,\,\mathrm{eff}}(t)}{\tau_{21}} - \frac{\Gamma_{\mathrm{s}}\sigma_{\mathrm{e}}c}{n_{\mathrm{c}}}\left[f_{\mathrm{us}}N_{2,\,\mathrm{eff}}(t) - f_{\mathrm{ls}}N_{1,\,\mathrm{eff}}(t)\right]\Phi(t) \\ & - \gamma_2 N_{2,\,\mathrm{eff}}(t),\end{aligned} \tag{6}$$

$$\frac{\mathrm{d}N_{1,\,\mathrm{eff}}(t)}{\mathrm{d}t} = -\frac{\mathrm{d}N_{2,\,\mathrm{eff}}(t)}{\mathrm{d}t}, \tag{7}$$

$$\begin{aligned}\frac{\mathrm{d}\Phi(t)}{\mathrm{d}t} = {} & -\frac{l_{\mathrm{f}}\Gamma_{\mathrm{s}}\sigma_{\mathrm{s}}c}{l_{\mathrm{c}}n_{\mathrm{c}}}\left[f_{\mathrm{us}}N_{2,\,\mathrm{eff}}(t)\right. \\ & \left. - f_{\mathrm{ls}}N_{1,\,\mathrm{eff}}(t)\right]\Phi(t) - \frac{\Phi(t)}{\tau_{\mathrm{c}}} + S,\end{aligned} \tag{8}$$

where Γ_{p} and Γ_{s} are the overlapping integral of pump mode and laser mode with the fiber core, respectively, and they can be calculated using the fiber core radius r_{c}, the numerical aperture of fiber core NA_{c}, the pump wavelength λ_{p} and the laser wavelength λ_{s} [13]; σ_{a} and σ_{e} are the absorption cross section and the stimulated emission cross section in the lasing process, respectively; ε(t) is the pump pulse shape as a function of time; the term $P_{\mathrm{a,eff}}$ ε(t) represents the temporal pump peak power; A_{c}, h, c and n_{c} are the cross-sectional area of the fiber core, the Planck constant, the speed of light in vacuum and the core refractive index of the fiber, respectively; ν_{p} is the optical frequency of the pump source which can be given by

$$\nu_{\mathrm{p}} = c/\lambda_{\mathrm{p}}; \tag{9}$$

Φ is the cavity photon density; τ_{21} is the spontaneous transition lifetime; γ_2 is the nonradiative transition rates; l_{c} is the length of the laser cavity; and τ_{c} is the cavity photon lifetime which can be given by [8, 9]

$$\tau_{\mathrm{c}} = \frac{2n_{\mathrm{c}}l_{\mathrm{c}}}{c[-\ln(R_1R_2) + 2\alpha_{\mathrm{s}}l_{\mathrm{c}} + 2\delta]}, \tag{10}$$

where R_1 and R_2 are the reflectivity of the input mirror and the output coupler (OC), respectively; α_{s} is the core absorption coefficient of the silica fiber at the lasing wavelength; and δ is the fusion loss introduced by fiber splicing; S is the rate at which spontaneous emission is contributed to the laser emission, and it can be given by [8]

$$S = \frac{\beta N_{2,\,\mathrm{eff}}(t) l_{\mathrm{f}}}{\tau_{21} l_{\mathrm{c}}}, \tag{11}$$

where β is the coupling ratio factor which is the ratio of the bandwidth of laser output $\Delta\nu_s$ and the bandwidth of spontaneous emission $\Delta\nu_{spe}$; f_{up} and f_{lp} are the Boltzmann factors of the upper and lower pump levels, respectively; f_{us} and f_{ls} are the Boltzmann factors of the upper and lower laser levels, respectively. According to the McCumber formula [14], they can be obtained that

$$f_{up}/f_{lp} = \sigma_e(\lambda_p)/\sigma_a(\lambda_p), \tag{12}$$

$$f_{ls}/f_{us} = \sigma_a(\lambda_s)/\sigma_e(\lambda_s), \tag{13}$$

$$\sigma_a(\lambda_p) = f_{lp}\sigma_a, \tag{14}$$

$$\sigma_e(\lambda_s) = f_{us}\sigma_e, \tag{15}$$

where $\sigma_a(\lambda_p)$, $\sigma_e(\lambda_p)$, $\sigma_a(\lambda_s)$ and $\sigma_e(\lambda_s)$ are the absorption cross section and the stimulated emission cross section at the pump wavelength λ_p and the laser wavelength λ_s, respectively. We assumed that

$$\chi_p = 1 + f_{up}/f_{lp}, \tag{16}$$

$$\chi_s = 1 + f_{ls}/f_{us}. \tag{17}$$

We can combine Eqs. (5, 6, 8, 12–17) to obtain the rate equations for our model

$$\begin{aligned}\frac{dN_{2,\,eff}(t)}{dt} &= \frac{\Gamma_p\sigma_a(\lambda_p)P_{a,\,eff}\varepsilon(t)}{A_c h\nu_p}\left[N_{0,\,eff}(t) - \chi_p N_{2,\,eff}(t)\right] - \frac{N_{2,\,eff}(t)}{\tau_{21}} \\ &- \frac{\Gamma_s\sigma_e(\lambda_s)c}{n_c}\left[\chi_s N_{2,\,eff}(t) - (\chi_s - 1)N_{0,\,eff}(t)\right]\Phi(t) - \gamma_2 N_{2,\,eff}(t),\end{aligned} \tag{18}$$

$$\begin{aligned}\frac{d\Phi(t)}{dt} &= -\frac{l_f\Gamma_s\sigma_e(\lambda_s)c}{l_c n_c}\left[\chi_s N_{2,\,eff}(t) - (\chi_s - 1)N_{0,\,eff}(t)\right]\Phi(t) \\ &- \frac{\Phi(t)}{\tau_c} + S.\end{aligned} \tag{19}$$

Thus, the temporal output power through the OC can be written as [9]

$$P_{out}(t) = \frac{\Phi(t)A_c c}{2n_c}\ln\left(\frac{1}{R_2}\right)h\nu_s, \tag{20}$$

where ν_s is the optical frequency of the laser output which can be given by

$$\nu_s = c/\lambda_s, \tag{21}$$

It should be noted that the effects introduced by the amplified spontaneous emission (ASE), the upconversion from $^3F_4$ level to higher energy level and the temperature of the gain medium are not considered in our theoretical model.

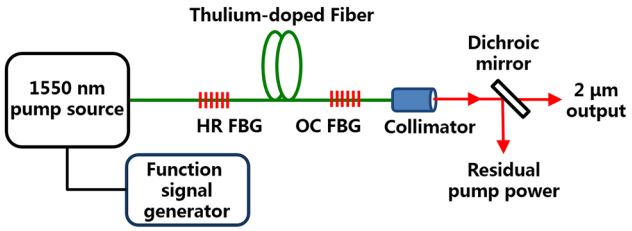

Fig. 1 Experimental setup of our IGSTDFL system

3 Experimental setup

The theoretical model was validated by comparing the numerical simulation results with the experimental results presented in our previous work [7]. The schematic of the experimental setup is depicted in Fig. 1, and the overview of this IGSTDFL is presented as follows.

The laser cavity consisted of three components: an input fiber Bragg grating (FBG) with high reflectivity (R_1 = 99 %) at laser wavelength, an output fiber Bragg grating (FBG) with partial reflectivity (R_2 = 30 %) at laser wavelength and a 25-cm polarization-maintaining TDF; the total length of the laser cavity was 55 cm. The laser system was pumped by a pulsed 1550-nm erbium-doped fiber laser with its maximum average pump power of 2 W. The pump source produced 100-ns square pulses with both its rising edge and falling edge being 5 ns at a repetition rate of 100 kHz; its pulse shape was driven by a function signal generator. A dichroic mirror was used to separate the laser output from residual pump power.

4 Numerical simulation results and discussion

A Runge–Kutta method was employed to solve the time-dependent rate equations in the numerical simulation. Part of parameters used in the numerical model is listed in Table 1, and others can be found in our experimental setup in Sect. 3. All numerical simulation results presented in this section are based on the theoretical model mentioned in Sect. 2 and these parameters unless stated otherwise.

Typical numerical results with respect to the evolution of the effective upper-level population density and the temporal output power are presented in Fig. 2a, b, respectively. As shown in Fig. 2a, since the lifetime of the $^3F_4$ level is much shorter than the period of the pump pulse, the upper-level population depletes slowly and remains in a nearly constant value after the lasing process. Therefore, although the threshold of the population inversion N_{th} can be obtained by solving the equation $d\Phi/dt = 0$, it is a problem to define the threshold of the pump power in our theoretical model.

Table 1 Parameters used in the numerical model

Parameter	Unit	Value	Offered by
N_0	m^{-3}	1.5×10^{26}	Nufern Inc.
λ_p	nm	1550	[7]
λ_s	nm	1926.7	[7]
$\alpha(\lambda_p, N_0)$	m^{-1}	12.474	Nufern Inc.
Γ_p	–	0.929	–
Γ_s	–	0.836	–
r_c	μm	5	Nufern Inc.
NA_c	–	0.15	Nufern Inc.
τ_{21}	μs	1395	[15]
γ_2	s^{-1}	2592.88	[16]
n_c	–	1.456	–
α_s	m^{-1}	2.3×10^{-3}	[17]
δ	–	0.02	–
β	–	10^{-8}	–
$\sigma_a(\lambda_p)$	m^2	1.50×10^{-25}	[18]
$\sigma_e(\lambda_p)$	m^2	0.10×10^{-25}	[18]
$\sigma_a(\lambda_s)$	m^2	0.42×10^{-25}	[18]
$\sigma_e(\lambda_s)$	m^2	4.50×10^{-25}	[18]
P_a	W	2	–

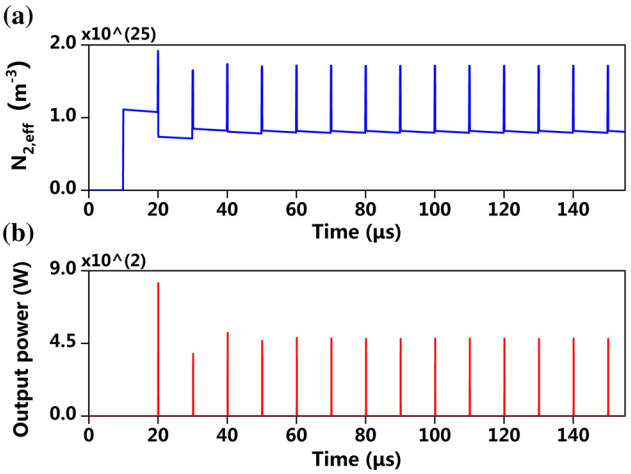

Fig. 2 Evolution of **a** the effective upper-level population density and **b** temporal output power achieved from the numerical simulation with typical parameters

Despite this, we can overlap the calculated output pulses to validate their stability and obtain the mean values of the pulse duration, the pulse peak power and hence the pulse energy which can represent their characteristics in this case. As shown in Fig. 2a, b, the laser system operates in an unstable regime in the first few periods; thus, the numerical simulation should be operated in sufficient periods, and the first few laser pulses should be ignored in the calculation.

We first considered the influence introduced by the average pump power to the features of output pulses in the laser system and verified our theoretical model by comparing the numerical simulation results with the experimental results [7]. The output pulse duration and the output pulse energy as the functions of average pump power are shown in Fig. 3a. It can be found that both the simulated pulse duration and pulse energy exhibit similar trends with the measured data as the pump power increases. The simulation results with shorter pulse duration and higher pulse energy compared with the experimental data can be attributed to the reasonable inaccuracies caused by those approximations in our theoretical model and/or the cavity losses which are not taken into account in the model, such as the coupling loss between the passive fiber and the TDF. Despite this slight deviation, the numerical simulation results are in good agreement with the measured data, confirming that our theoretical model is effective for further investigation of the IGSTDFL. As shown in Fig. 3a, the laser pulse energy is nearly proportional to the average pump power, while the laser pulse duration is almost inversely proportional to the average pump power; these phenomena are consistent with those IGSTDFL experiments until the thermal effects or gain saturation occurs [5–7]. This indicates that the output pulse duration of the IGSTDFL can be shortened by increasing the average pump power. However, when the average pump power reaches a high level in our simulation, the laser system produces output pulses with trailing edge (Fig. 4b) or relaxation oscillation (RO) spikes (Fig. 4c), and these pulse distortion effects can also be found in several IGSTDFL systems and other gain-switched lasers [4, 19]. Comparing Fig. 4b, c with Fig. 4a, we can find that these phenomena are caused by the large pump rate compared with the pump pulse duration, and thus, the photon density reaches its peak before the pump pulse ends; their physical mechanism can be found in detail in Ref. [8].

When the IGSTDFL operates for practical applications, the state in which output pulses with trailing edge or RO spikes are produced should be circumvented. According to our theoretical model and numerical simulation, we obtained the pump condition in which the IGSTDFL produces pulses with Gaussian shape; the result is shown in Fig. 3b. It should be noted that the pulse distortion phenomena are more likely to occur when the pulse duration is long and the average pump power is high, which is consistent with their mechanisms. In addition, in gain-switched TDFL systems, self-starting mode-locked-like sub-pulses can be observed within an envelope of a gain-switched pulse when the pump pulse energy is large [6, 20–22]. These phenomena may be attributed to several mechanisms including excited-state absorption (ESA) and interactions between longitudinal modes [22–24]. In our model, upper energy levels ($^3H_4$ and $^3H_5$) are not included, and only monochromatic lasing operation is considered. Therefore,

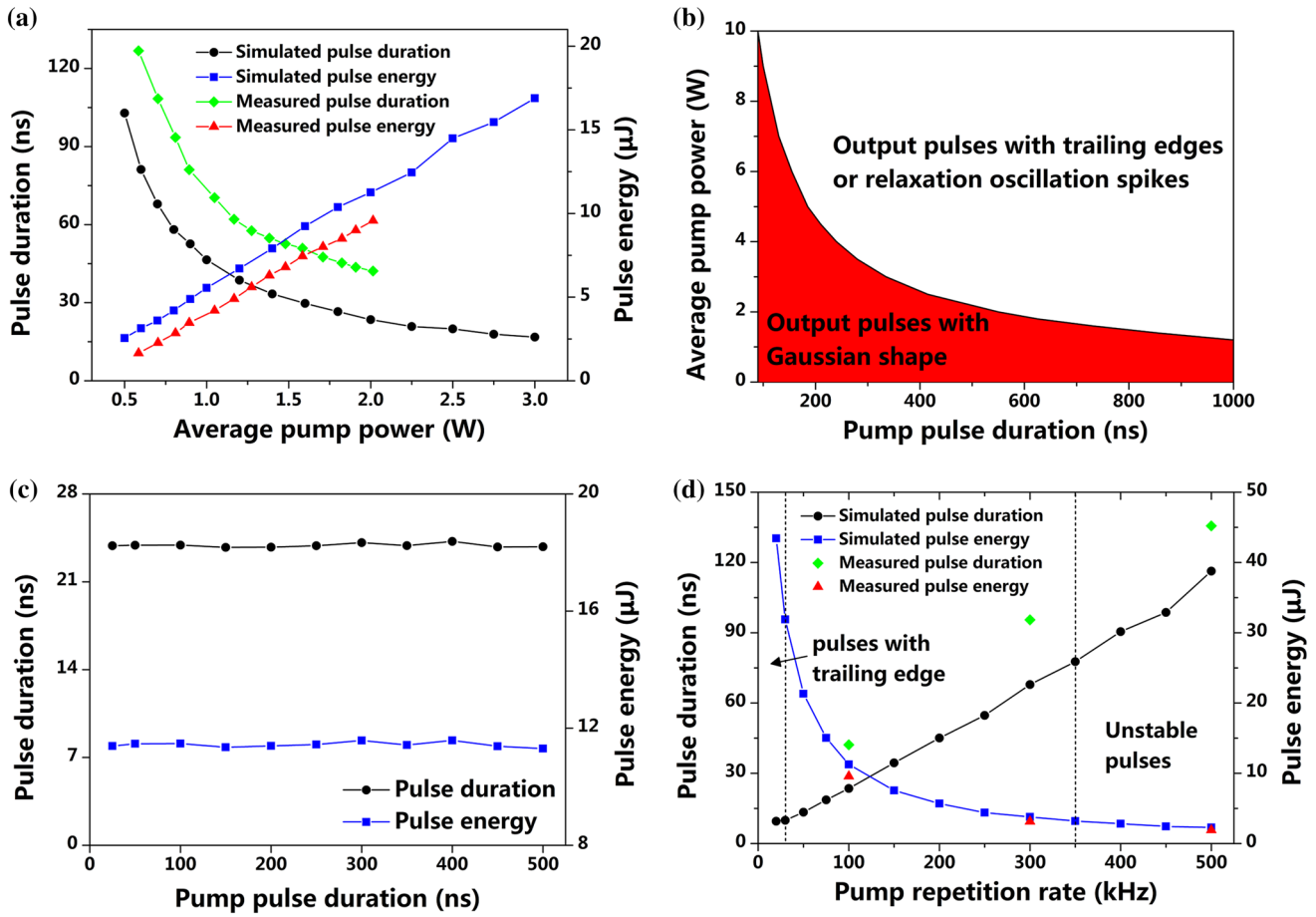

Fig. 3 Output pulse duration and output pulse energy versus **a** the average pump power, **c** the pump pulse duration, **d** the pump repetition rate; **b** the pump condition in which the laser produces output pulses with Gaussian shape (*red region*) or with trailing edge and relaxation oscillation spikes (*white region*)

the ESA effect, longitudinal mode interactions and hence the self-starting mode-locked pulse phenomena cannot be predicted by the simulation, which limits the use of this model in the laser systems with high pump pulse energy.

As shown in Fig. 3c, the output pulse duration and pulse energy remain relatively stable until the pulse distortion occurs. These results indicate that the pump pulse duration should not be first considered when attempting to achieve short pulses with high pulse energy in the IGSTDFL system unless the relaxation oscillations are induced. Figure 3d illustrates the output pulse duration and output pulse energy versus the pump repetition rate, respectively; both the experimental data [7] and the simulation results are included. According to Fig. 3d, we can find that the simulated result of the pulse energy is in good agreement with the measured data. The simulated pulse durations are slightly longer than the measured durations due to the inaccuracy mentioned above, further indicating that our theoretical model is effective and can be supported by the experimental data. As shown in Fig. 3d, with a fixed pump power, the IGSTDFL system generates pulses with distortion effects when the pump repetition rate is low, while it generates unstable pulses when the pump repetition rate is high. Thus, higher pump pulse energy is required for stable operation of the IGSTDFL with high repetition rate, and this inference from the simulation is confirmed by experimental results in [5, 7]. It could also be inferred from Fig. 3a, d that the pump repetition rate has opposite effects on the features of output pulses when compared with the average pump power.

In addition, the parameters of the cavity configuration, including the reflectivity of the OC, the length of the laser cavity and the length of the TDF, also have significant influences to the characteristics of the output laser pulses. Figure 5a illustrates the output pulse duration and output pulse energy versus the pump repetition rate at different average pump powers. It can be found that the output pulse duration and pulse energy exhibit similar trend under different pump conditions, respectively: With the increase in the OC reflectivity, the pulse duration decreases at first but

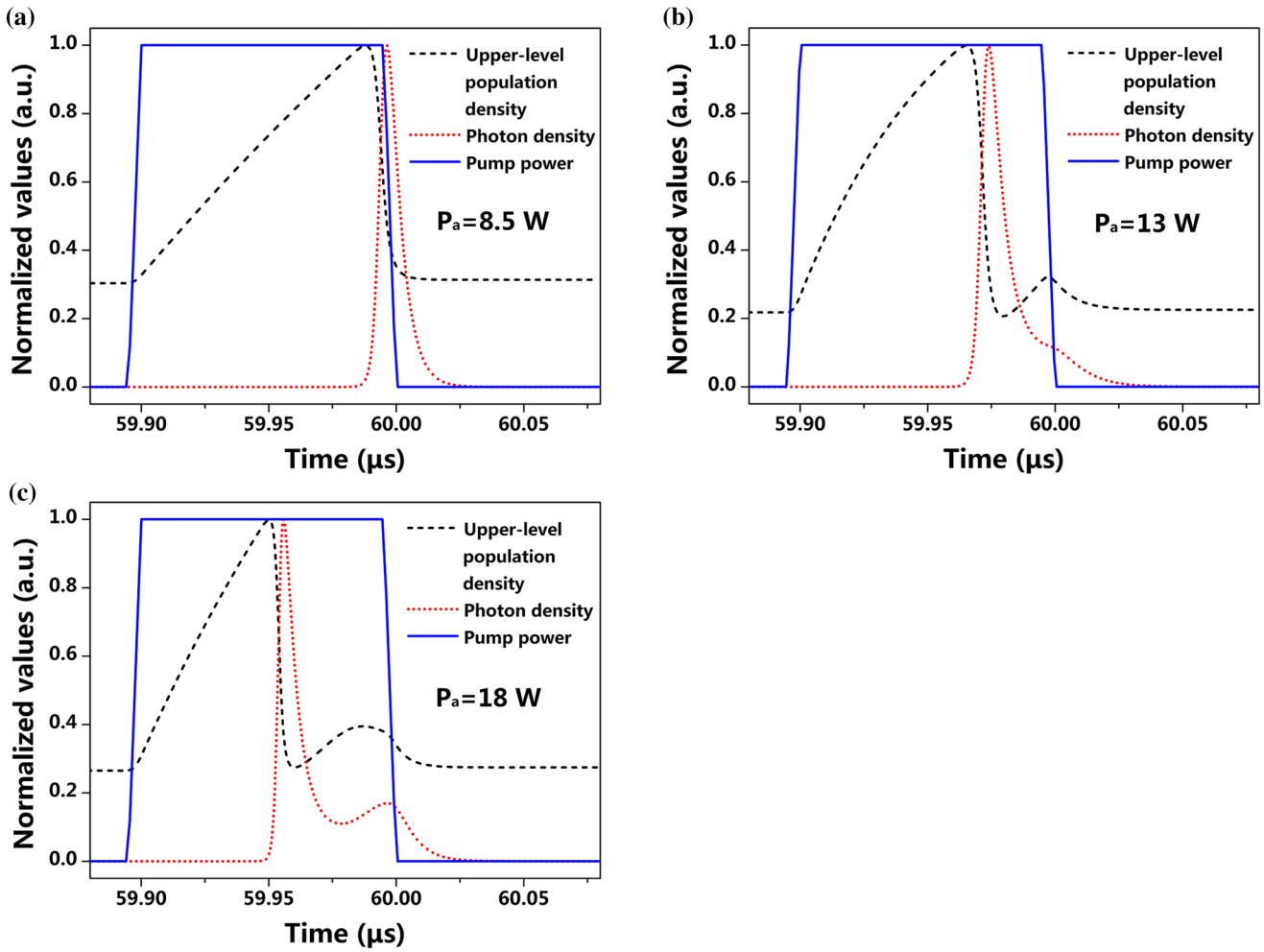

Fig. 4 Overlaps of the normalized pump pulse, upper-level population density and output pulse with **a** Gaussian shape, **b** trailing edge and **c** relaxation oscillation spike, at different average pump powers

then increases, and the pulse energy increases at first but then decreases; when the reflectivity of the OC is high, the pulse distortion occurs. However, the minimum pulse duration and the maximum pulse energy cannot be achieved simultaneously under identical pump condition, and each of them varies under different pump conditions. These numerical results indicate two principles for the optimization of the OC reflectivity in the IGSTDFL system: (1) the pump condition should be taken into account and (2) there should be a trade-off between the minimum output pulse duration and the maximum output pulse energy according to the requirements of different practical applications.

Since our theoretical model is based on an IGSTDFL system with all-fiber configuration, both the length of the passive fiber and the length of the TDF are contributed to the laser cavity length. We first considered the cavity length only with the change in passive fiber length; the TDF fiber length and hence the gain provided by the first term on the right-hand side of Eq. (18) remained constant. The numerical results are shown in Fig. 5b. It can be found that the change in cavity length has little influence to the output pulse energy. According to Eq. (10), this phenomenon can be physically analyzed by the fact that the lasing wavelength absorption loss related to the cavity length (~10^{-3}) is negligible when compared with the output coupling loss (~1) in our numerical model. As shown in Fig. 5b, the output pulse duration is almost in proportion to the cavity length, implying that shorter output pulse duration can be achieved by reducing the laser cavity length, especially the length of passive fiber; this result is also confirmed by a systematic study in Ref. [4].

Figure 5c presents the output pulse duration and the output pulse energy as the functions of the TDF length. The process in which output pulse duration and output pulse energy change with the increase in TDF length can be divided into two main stages: At first, the pulse duration decreases rapidly and the pulse energy has noticeable growth when the TDF length is <0.2 m, and then the pulse

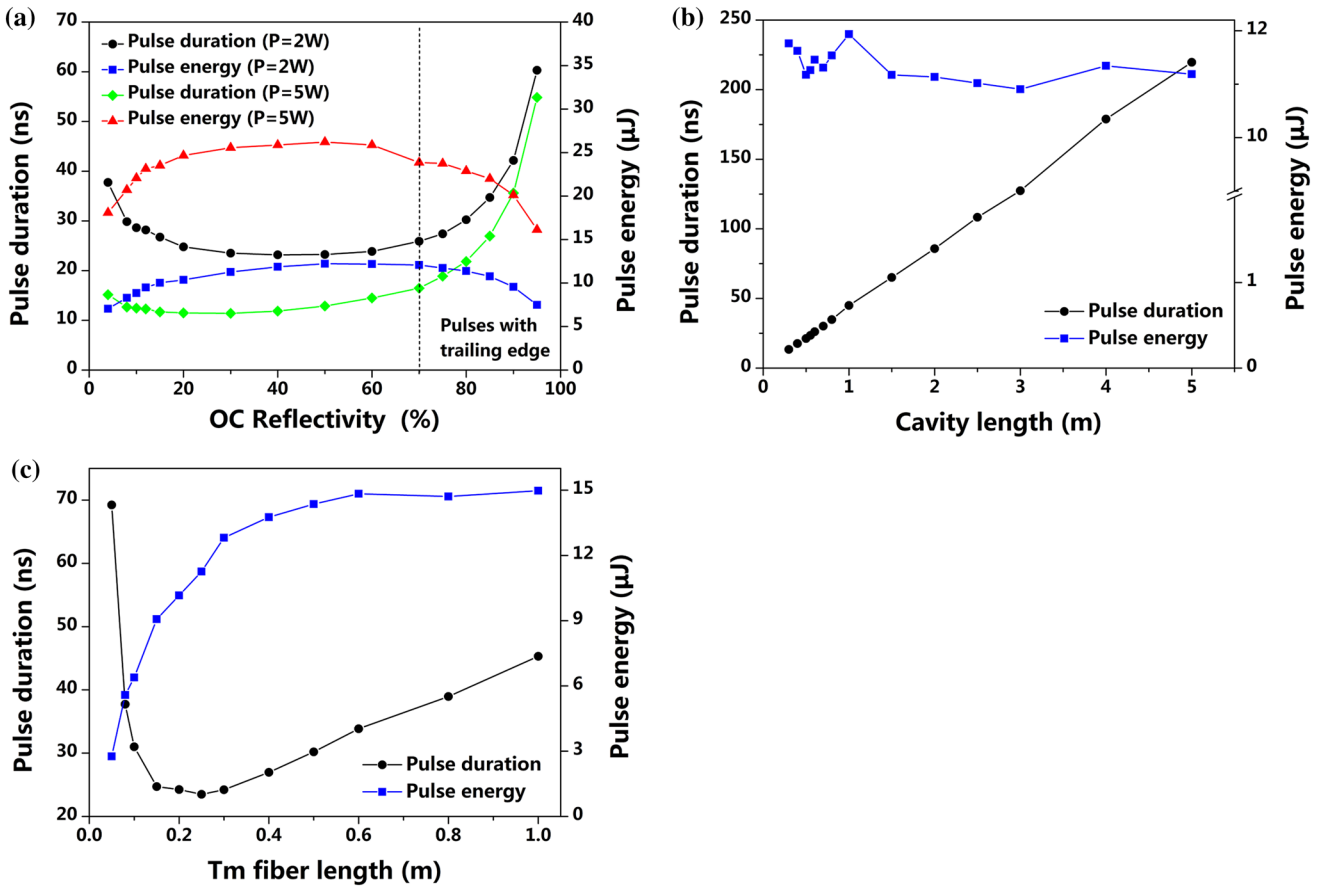

Fig. 5 Simulated output pulse duration and output pulse energy versus **a** the reflectivity of output coupler at different average pump power, **b** the cavity length which is changed by the length of passive fiber and **c** the length of the thulium-doped fiber

duration increases slowly while the growth of the pulse energy slows down. In the first stage, the pump power absorption is reduced due to shorter length of the TDF, and the absorption increases from 46.40 % at 0.05 m to 91.75 % at 0.2 m; the rate of upper-level population accumulation increases more rapidly with the increase in the TDF length and hence the shorter photon buildup time, which results in rapid increase in pulse energy and decrease in pulse duration. In the second stage, most of the pump power is absorbed; the absorption only increases by 8.24 % from 91.75 % at 0.2 m to 99.99 % at 1.0 m, and thus, the growth of the pulse energy slows down and the pulse duration increases since the cavity length becomes longer. Therefore, the TDF length should be carefully designed in the IGSTDFL system because shorter TDF introduces poor pump absorption, while longer TDF results in longer pulse duration.

We did not consider the influence of the Tm^{3+}-ions-doping concentration in our numerical model because we did not obtain the absorption coefficients $\alpha(\lambda_p, N_0)$ of other TDFs with different concentrations.

5 Conclusion

In summary, we have demonstrated an effective and simple theoretical model of the IGSTDFL system. The model is based on the time-dependent rate equations in which spatial variables are approximated by the defined effective pump power and effective population density. We validated our model by comparing the numerical simulation results with the experimental data from our previous work; good agreement has been obtained. The numerical results from our theoretical model were further investigated to optimize the IGSTDFL system for the purpose of achieving stable output pulses with short duration and high pulse energy. The parameters of the pump source and the cavity geometry were considered in the optimization; the pump condition in which the pulse distortion occurs was presented. We believe that our model can be expanded to other gain-switched fiber laser setups. Future work will focus on the improvement of this model for the discussion of self-mode-locking mechanisms and the theoretical model of the mode-locked TDFLs.

Acknowledgments The authors would like to acknowledge Advanced Fiber Resources (Zhuhai) Ltd. for the technical support in this work. Special thanks to Dingxiang Cao, Deping Zhao and Qian Fu for helpful discussion. This work was partially supported by the National Natural Science Foundation of China under Grants 61308056, 11204044, 11232015 and 11072271, the Research Fund for the Doctoral Program of Higher Education of China under Grants 20120171110005 and 20130171130003 and the Fundamental Research Funds for the Central Universities of China under Grant 14lgpy07.

References

1. N.J. Scott, C.M. Cilip, N.M. Fried, IEEE J. Sel. Top. Quantum Electron. **15**(2), 435–440 (2009)
2. G.J. Koch, J.Y. Beyon, B.W. Barnes, M. Petros, J. Yu, F. Amzajerdian, M.J. Kavaya, U.N. Singh, Opt. Eng. **46**, 116201–116214 (2007)
3. D. Creeden, P.A. Ketteridge, P.A. Budni, S.D. Setzler, Y.E. Young, J.C. McCarthy, K. Zawilski, P.G. Schunemann, T.M. Pollak, E.P. Chicklis, M. Jiang, Opt. Lett. **33**(4), 315–317 (2008)
4. M. Jiang, P. Tayebati, Opt. Lett. **32**(13), 1797–1799 (2007)
5. N. Simakov, A. Hemming, S. Bennetts, J. Haub, Opt. Express **19**(16), 14949–14954 (2011)
6. J. Swiderski, M. Maciejewska, J. Kwiatkowski, M. Mamajek, Laser Phys. Lett. **10**(1), 015107 (2013)
7. Z. Jiao, B. Zhang, B. Wang, Opt. Laser Technol. **55**, 58–61 (2014)
8. W. Koechner, *Solid-state Laser Engineering* (Springer, Berlin, 2013)
9. O. Svelto, *Principles of Lasers* (Springer, Berlin, 2010)
10. F. Wang, D. Shen, H. Chen, D. Fan, Q. Lu, Opt. Rev. **18**(4), 360–364 (2011)
11. R. Zhou, Y. Ju, J. Zhao, C. Yang, Y. Wang, Chin. Phys. B **22**(6), 064208 (2013)
12. J. Yang, H. Li, Y. Tang, J. Xu, J. Opt. Soc. Am. B **31**(1), 80–86 (2014)
13. A. Yariv, P. Yeh, *Photonics: Optical Electronics in Modern Communications* (Oxford University Press, Oxford, 2007)
14. D.E. McCumber, Phys. Rev. **134**(2A), A299 (1964)
15. B. Peng, T. Izumitani, Opt. Mater. **4**(6), 797–810 (1995)
16. R. Reisfeld, M. Eyal, Le Journal de Physique Colloques **46**(C7), C7–349 (1985)
17. S.D. Jackson, T.A. King, J Lightwave Technol **17**(5), 948–956 (1999)
18. S.D. Agger, J.H. Povlsen, Opt. Express **14**(1), 50–57 (2006)
19. V. Agrez, R. Petkovsek, Appl. Opt. **52**, 3066–3072 (2013)
20. J. Swiderski, M. Michalska, Opt. Lett. **38**(10), 1624–1626 (2013)
21. J. Swiderski, M. Michalska, C. Kieleck, M. Eichhorn, G. Mazé, IEEE Photonics Technol. Lett. **26**(2), 150–153 (2014)
22. H.-X. Tsao, C.-H. Chang, S.-T. Lin, J.-K. Sheu, T.-Y. Tsai, Opt. Laser Technol. **56**, 354–357 (2013)
23. F.Z. Qamar, T.A. King, J. Mod. Opt. **52**(7), 1031–1043 (2005)
24. F.Z. Qamar, T.A. King, J. Mod. Opt. **52**(8), 1053–1063 (2005)